Essential role of TNF receptor superfamily 25 (TNFRSF25) in the development of allergic lung inflammation

Lei Fang, Becky Adkins, Vadim Deyev, and Eckhard R. Podack

Department of Microbiology and Immunology, Leonard Miller School of Medicine, University of Miami, Miami, FL 33136

We identify the tumor necrosis factor receptor superfamily 25 (TNFRSF25)/TNFSF15 pair as critical trigger for allergic lung inflammation, which is a cardinal feature of asthma. TNFRSF25 (TNFR25) signals are required to exert T helper cell 2 (Th2) effector function in Th2-polarized CD4 cells and co-stimulate interleukin (IL)-13 production by glycosphingolipid-activated NKT cells. In vivo, antibody blockade of TNFSF15 (TL1A), which is the ligand for TNFR25, inhibits lung inflammation and production of Th2 cytokines such as IL-13, even when administered days after airway antigen exposure. Similarly, blockade of TNFR25 by a dominant-negative (DN) transgene, DN TNFR25, confers resistance to lung inflammation in mice. Allergic lung inflammation–resistant, NKT-deficient mice become susceptible upon adoptive transfer of wild-type NKT cells, but not after transfer of DN TNFR25 transgenic NKT cells. The TNFR25/TL1A pair appears to provide an early signal for Th2 cytokine production in the lung, and therefore may be a drug target in attempts to attenuate lung inflammation in asthmatics.

CORRESPONDENCE
Eckhard R. Podack:
epodack@miami.edu

Abbreviations used: HE, hematoxylin and eosin; PAS, periodic acid-Schiff; tg, transgenic; TNFRSF, TNF receptor superfamily.

TNF receptor superfamily 25 (TNFRSF25 [TNFR25]) was cloned by several groups under the names Wsl-1, Apo3, LARD, TRAMP, DR3, and TR3 (1–6) as a member of the TNF-receptor family with a typical death domain. Transfected TNFR25 has been shown to induce rapid apoptosis by activating the caspase cascade through interaction with TRADD and FADD (4, 7, 8). Like other TNF receptor family members, TNFR25 is also able via TRADD and TRAF2 to induce NF-κB and promote cell survival signals (2, 5, 9–12). TNFR25 is expressed constitutively in the form of randomly spliced transcripts, primarily in lymphoid cells (2, 3, 13) but also in other cells, including tumor cells (6, 14).

The ligand for TNFR25 has recently been identified as TL1A (TNFSF15) (11). TL1A has co-stimulatory activity for TNFR25-expressing T cells through the activation of NF-κB and suppression of apoptosis by up-regulation of c-IAP2 (12). TL1A expression is detected on human umbilical vein endothelial cells and mediates antiangiogenic activity (15). Up-regulated expression of TL1A is also found on macrophages and lymphocytes in human inflammatory bowel disease and correlated with the severity of inflammation, implying that TL1A/TNFR25 signals may be involved in inflammatory bowel disease (16, 17). TL1A synergizes with IL-12 and -18 to promote IFN-γ production in human T cells and NK cells (18). Whether TL1A/TNFR25 signals play a role in Th2-mediated functions and disease pathology has not been investigated.

Germ line deletion of TNFR25 in mice displayed a partial defect in negative selection of thymocytes; however, no phenotypic changes were observed in TNFR25-deficient peripheral T cells compared with WT cells (19).

Allergic, atopic lung inflammation is thought to be one of the underlying causes for airway hyperreactivity and asthma. It is characterized by IL-13 production by NKT and T cells; by Th2 polarization of CD4 cells associated with elevated IgE levels; by cellular, prominently eosinophilic, infiltration into the peribronchial space and bronchoalveolar fluid; and by goblet cell hyperplasia and increased mucus production (20–24). In this study, we show that TNFR25 is a molecular trigger for amplified Th2 cytokine production by polarized CD4 cells and for IL-13 production by NKT cells, and that blockade of TNFR25 inhibits allergic lung inflammation, a cardinal feature of asthma, in murine models.

The Rockefeller University Press $30.00
J. Exp. Med. Vol. 205 No. 5 1037-1048 www.jem.org/cgi/doi/10.1084/jem.20072528

The Journal of Experimental Medicine

RESULTS

TNFR25 is constitutively expressed on NKT cells and co-stimulates IL-13 production

To study the biological functions of TNFR25 and its cognate ligand TL1A, hamster anti–mouse monoclonal antibodies to TNFR25 were generated by standard protocols and used to measure TNFR25 expression by flow cytometry on primary lymph node and spleen cells. TNFR25 was detected at low levels on naive CD4 T cells, and at even lower levels on CD8 T cells. In contrast, NKT cells expressed high levels of TNFR25 (Fig. 1 A). A subpopulation of $CD11c^+$ cells and NK cells were also TNFR25 positive, whereas B cells were negative. We confirmed previous data that activated CD4 and CD8 T cells up-regulated TNFR25 expression (unpublished data) (13). In the thymus, single-positive CD4 and CD8 cells expressed TNFR25 at levels similar to naive peripheral T cells. CD4/CD8 double-positive and -negative thymocytes did not express TNFR25 (unpublished data). The high level of constitutive TNFR25 expression on NKT cells suggested that TNFR25 may have important functions in NKT co-stimulation.

NKT cells are early mediators of immune responses by rapidly secreting IFN-γ or IL-13/IL-4. NKT cells have been implicated in Th1/Th2 polarization and in the pathogenesis of lung inflammation (25), autoimmunity, and antitumor immunity (26–29). Using an agonistic anti-TNFR25 antibody (4C12), we determined whether signals emanating from TNFR25 on NKT cells had effects on their secretion of Th1 or Th2 cytokines. NK/NKT cells were enriched from pooled spleen cells of 10 mice by positive selection

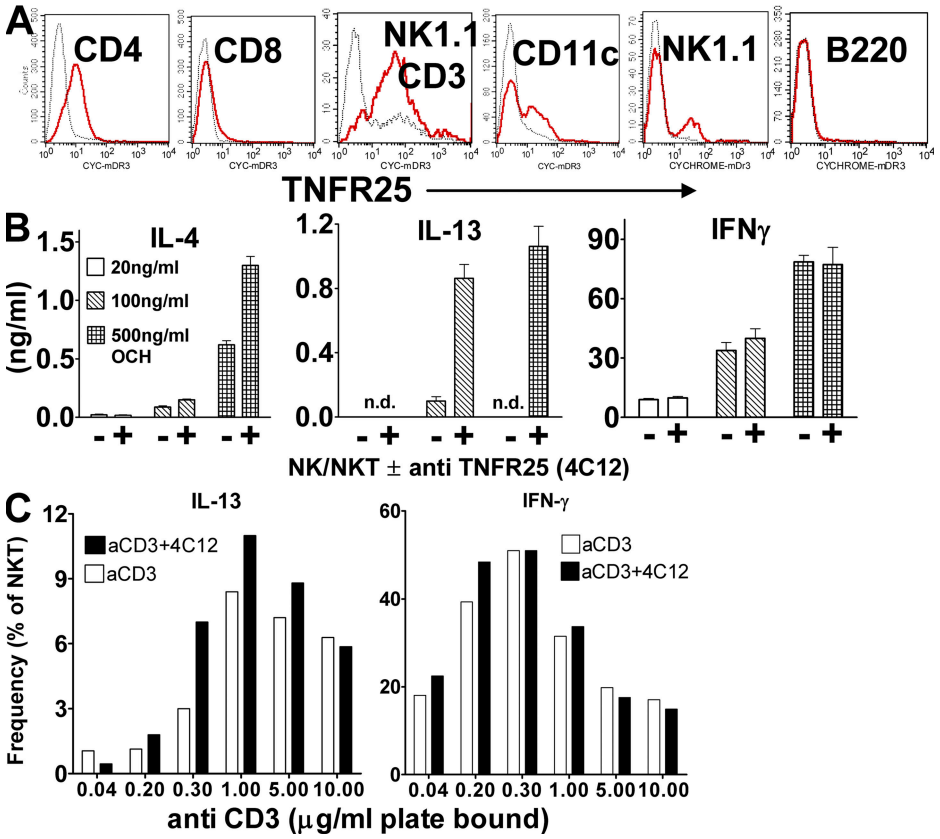

Figure 1. TNFR25 is constitutively expressed on resting NKT cells and co-stimulates IL-4 and -13 cytokine production. (A) Expression of TNFR25 in lymph node cells. Cells were gated for CD4, CD8, B220, CD11c, or NK1.1-positive and CD3-negative cells or NK1.1/CD3 double-positive cells and TNFR25 fluorescence displayed in the histogram. Red curve, anti-TNFR25; black curve, isotype control. (B) TNFR25 co-stimulation of IL-4 and -13 production by glycosphingolipid-activated NKT cells. NKT cells were enriched from pooled spleen cells from 10 mice by positive selection using the EasySep mouse Pan NK Positive Selection kit. The ratio of NK to NKT cells in the enriched population was 65:35 × 10^5 cells were incubated for 48 h in flat bottom 96-microtiter plates in triplicate in the presence of 10 ng/ml IL-15 and stimulated with 20, 100, or 500 ng/ml OCH-glycosphingolipid. Co-stimulation was achieved with 5 μg/ml agonistic anti-TNFR25 antibody 4C12 as indicated; cytokines were analyzed in supernatants by ELISA. n.d., not detectable. Representative of three independent experiments. (C) TNFR25 co-stimulation increases the frequency of IL-13–producing NKT cells. Enriched NK/NKT cells purified as described above were incubated with increasing concentrations of plate-bound anti-CD3, as indicated in the presence and absence of 5 μg/ml agonistic anti-TNFR25 (4C12) for 72 h. Details of the method for intracellular cytokine staining are given in Materials and methods. In negative controls for unspecific staining, anti–IL-13 was blocked with recombinant IL-13 before use in intracellular staining (see Materials and methods) and were given values of <1%. Data for intracellular staining of IL-13 and IFN-γ in NKT cells were obtained by gating on NK1.1 and CD3 double-positive cells. Data are taken from two experiments. Error bars represent the mean ± the SEM.

using a mouse pan-NK-Positive Selection kit (StemCell Technologies), resulting in a population composed of 65% NK and 35% NKT cells. NK cells express CD1d and therefore are able to present lipids to the TCR of invariant NKT cells. NKT cells were stimulated with increasing concentrations of the glycosphingolipid OCH or with anti-CD3,

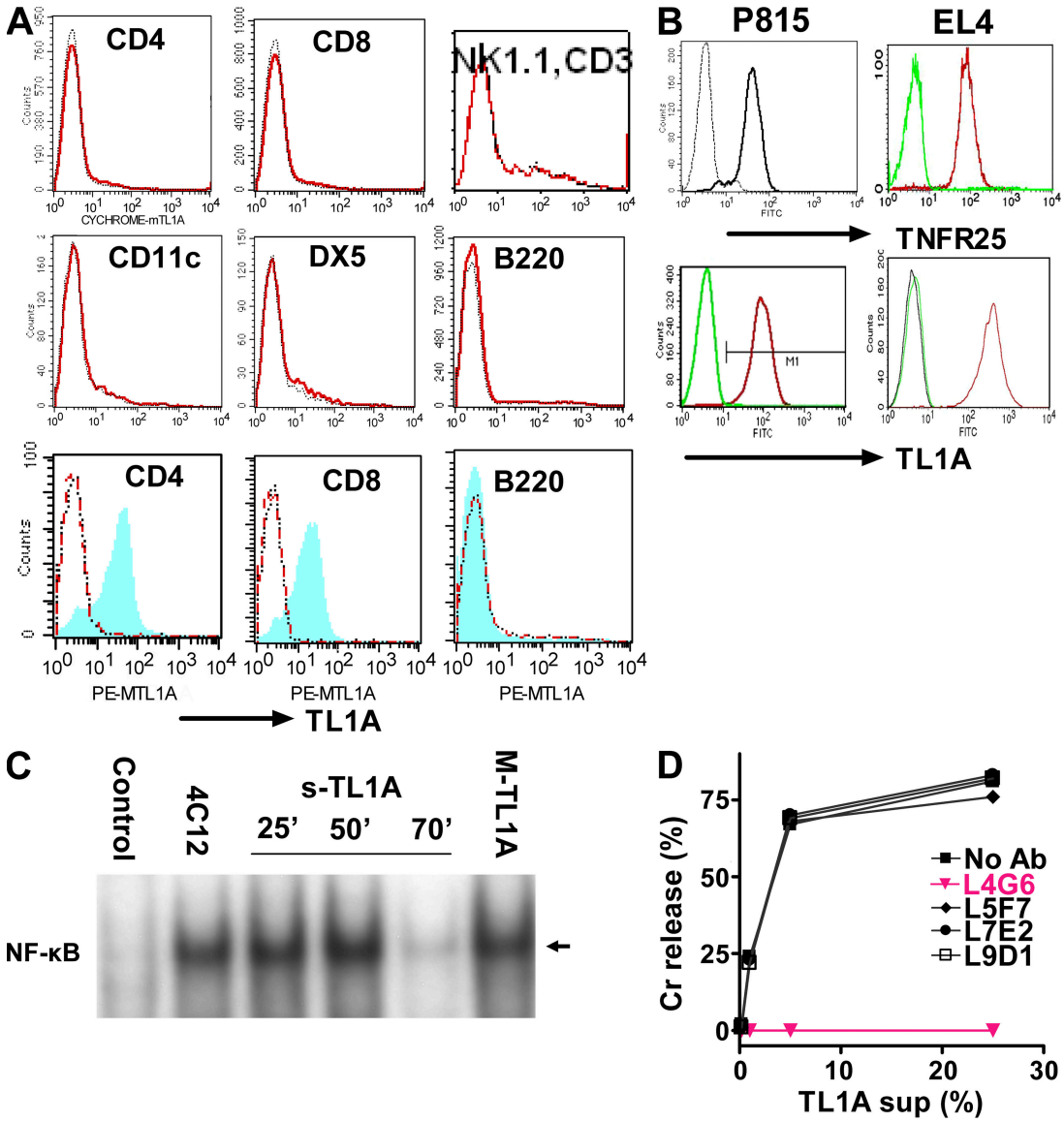

Figure 2. TL1A–triggered TNFR25 signals are blocked by antagonistic anti–TL1A L4G6. (A) TL1A is not expressed on resting lymphocytes and up-regulated on activated T cells (top 6 graphs). Resting splenocyte cell suspensions were gated using the respective labeled antibody as a population marker and the TL1A histogram displayed. Red curve, anti-TL1A; black curve, isotype control (bottom 3 graphs). Splenocytes were activated for 24 h with plate-bound anti-CD3 or with LPS and stained with anti-TL1A and with the population marker, as indicated. After gating on the population marker, TL1A expression on activated cells is shown as blue/shaded histogram. Red curve, resting cells; black curve, isotype control. Representative of more than three experiments. (B) TNFR25 and TL1A expression on cDNA transfected P815 and EL4. Transfected (right curve in each histogram) and untransfected cells were stained with the appropriate antibody and isotype controls and analyzed by flow cytometry. (C) TNFR25 activates NF-κB when triggered by agonistic antibody 4C12, by soluble TL1A or by membrane-bound TL1A. NF-κB activation was measured in EL4 cells transfected with TNFR25 in response to TNFR25 triggering. Cells were treated with the agonistic anti-TNFR25 antibody 4C12 (5 μg/ml) for 50 min; soluble TL1A was given for 25, 50, or 70 min, as indicated in the form of 25% supernatants from TL1A-transfected EL4 cells; membrane-bound TL1A (MTL1A) was given for 50 min by adding TL1A-transfected EL4-cells directly to TNFR25-transfected EL4. Controls received EL4 (untransfected) supernatants for 50 min. Nuclear extracts were prepared and analyzed by EMSA; the arrow indicates activated NF-κB. (D) Anti-TL1A antibody L4G6 blocks TL1A induced cell death of TNFR25-transfected cells. Soluble TL1A harvested from supernatants of P815-TL1A–transfected cells were mixed with ^{51}Cr-labeled P815-TNFR25 target cells. Different anti-murine TL1A monoclonal antibodies were added into the assay, and ^{51}Cr release was analyzed 5 h later. L4G6 antibody completely blocked the ability of TL1A to induce apoptosis in TNFR25-transfected P815 cells.

with and without co-stimulation of TNFR25 by the agonistic anti-TNFR25 antibody 4C12. OCH is a derivative of α-galactosylceramide with a shortened sphingosine chain. After 2 d of stimulation with increasing concentrations of OCH in the presence or absence of agonistic anti-TNFR25 (4C12), the supernatants were harvested and analyzed for IL-13, IL-4, and IFN-γ by ELISA (Fig. 1 B). TNFR25 signals co-stimulated lipid-dependent IL-13 production and, to a lesser extent, IL-4 production, but had no effect on IFN-γ production. In the absence of lipid, anti-TNFR25 alone did not induce production of any of the cytokines (unpublished data). TNFR25 signals also up-regulated the frequency of IL-13–secreting NKT cells, as detected by intracellular staining and gating on NK1.1/CD3 double-positive cells (Fig. 1 C). TNFR25-mediated IL-13 co-stimulation was most pronounced at an anti-CD3 concentration of 0.3–1 μg/ml, suggesting sensitivity of TNFR25 co-stimulation to antigen concentration. IFN-γ responses occur at lower anti-CD3 concentrations, but are not subject to TNFR25 co-stimulation.

TL1A is expressed on activated CD4 and CD8 T cells and activates NF-κB and apoptosis in TNFR25-transfected cells

To study the ligand for TNFR25, we generated monoclonal antibodies to murine TL1A for flow cytometry and functional studies. Resting lymph node cells are TL1A negative, including NKT and T cells, B cells, NK cells, and DCs (Fig. 2 A). After activation with anti-CD3 or LPS, respectively, CD4 and CD8 T cells express TL1A, whereas activated B cells remain TL1A negative. TL1A expression on activated T cells is transient and disappears after ∼48 h. All tissues analyzed, including lung, are TL1A negative when analyzed by PCR or flow cytometry. We set out to identify TL1A-blocking antibodies to generate tools to elucidate the in vivo function of TL1A–TNFR25 interaction.

TL1A-transfected tumor cells permanently express TL1A, which is detectable both as membrane-bound protein by flow cytometry (Fig. 2 B) and in cell-free supernatant as soluble TL1A by ELISA (not depicted) and by functional activity. Both soluble and membrane-bound TL1A are able to trigger TNFR25 signals (Fig. 2, C and D). Similar to TNF, membrane-bound and soluble TL1A activate NF-κB (Fig. 2 C) and induce apoptosis in TNFR25-transfected tumor cells (Fig. 2 D), as has been previously reported (1–6, 10). The anti-TNFR25 agonistic antibody 4C12 used in Fig. 1 B also activated NF-κB (Fig. 2 C) and mediated apoptosis of TNFR25-transfected tumor cells (not depicted).

We determined whether any of the anti-TL1A antibodies we had generated exhibited blocking activity for TL1A-mediated apoptosis of TNFR25-expressing targets. One of the anti-TL1A antibodies, L4G6, completely blocked TL1A-mediated lysis of TNFR25-transfected cells, whereas several other anti-TL1A antibodies had no effect (Fig. 2 D). Therefore, L4G6 antibody was selected for in vivo blockade of TL1A in genetically unmodified WT mice.

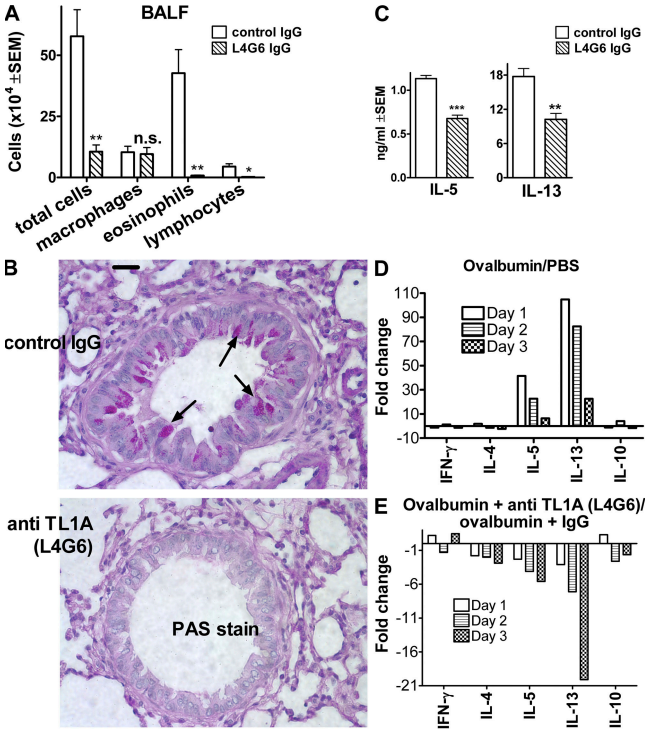

Figure 3. Antagonistic anti-TL1A antibody (L4G6) blocks lung inflammation. (A) Diminished cellular exudation in BALF in anti-TL1A (L4G6)–treated mice. Mice were primed i.p. on day 0 and 5 with 66 μg ovalbumin absorbed to alum. On day 12, mice were aerosol challenged with 0.5% ovalbumin in PBS for 1 h using an ultrasonic nebulizer. Mice received 4 daily doses of 50 μg purified L4G6-IgG i.p. (anti-TL1A), beginning 1 d before aerosol. Controls received the same amount and schedule of purified hamster IgG. All mice were analyzed 3 d after aerosol antigen exposure ($n = 4$; representative of >10 experiments). *, $P < 0.05$; **, $P < 0.01$. (B) TL1A-blocking antibody L4G6 suppresses mucus production and lung inflammation. Lung histology after PAS staining after treatment of mice with control IgG (top) or L4G6-IgG (anti-TL1A; bottom). Notice the lack of mucus production and cell infiltration in L4G6-treated animals (arrows point to mucus in mice treated with control IgG). Experiments were repeated three times. (C) Diminished IL-5 and -13 production by ovalbumin restimulated bronchial lymph node cells after TL1A blockade with L4G6. Bronchial lymph node cells were harvested 3 d after aerosol and restimulated in vitro with 100 μg/ml ovalbumin for 4 d. IL-4 was not detectable (not depicted), even in the absence of anti-TL1A. $n = 4$; **, $P < 0.01$; ***, $P < 0.001$. Experiments were repeated more than three times. (D) Cytokine expression in lung parenchyma after ovalbumin aerosol exposure. Lungs were harvested 1, 2, or 3 d after ovalbumin aerosol treatment. RNA was extracted, and after reverse transcription it was analyzed by Taqman PCR. Values are normalized to GAPDH cDNA and expressed as the fold increase of ovalbumin aerosol–treated over untreated mice. (E) Blocking anti-TL1A antibody L4G6 suppresses ovalbumin-induced cytokine expression in lung parenchyma. Mice were immunized twice with ovalbumin/alum, as described. 1 d before ovalbumin aerosol and for the next 3 d, mice received 50 μg blocking TL1A antibody L4G6 or control IgG i.p. Lungs were analyzed for expression of cytokine mRNA on day 1–3 after aerosol administration by Taqman PCR, as above. Data are presented as anti-TL1A–induced suppression of cytokine mRNA over control IgG.

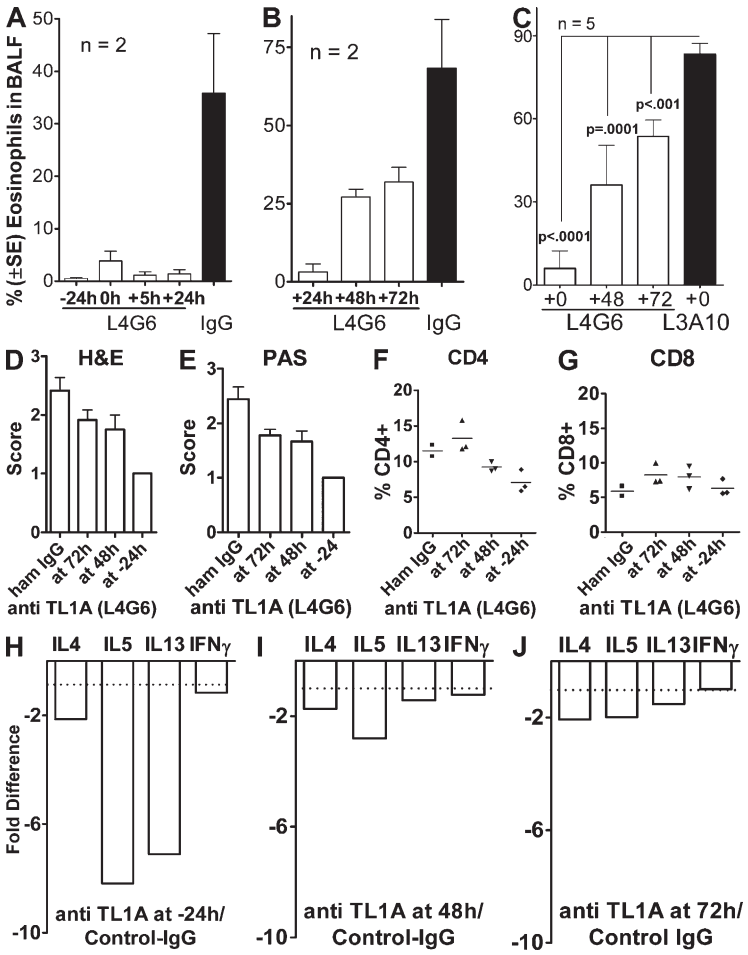

Figure 4. Kinetics of inhibition of lung inflammation by administration of blocking and nonblocking anti-TL1A. Mice were immunized and subjected to ovalbumin aerosol according to our standard protocol. Administration of 50 µg blocking (L4G6) or nonblocking (L3A10) anti-Tl1A, or control hamster IgG i.p. was started at the time indicated relative to aerosol exposure and continued daily until analysis, which was at 76 h after aerosol. In the 72-h time points, anti-TL1A was administered 4 h before analysis. A, B, and C are separate experiments testing different schedules and controls. Note that nonblocking TL1A (L3A10) does not affect eosinophil exudation, similar to hamster IgG. (A and B) Data from three experiments with two mice. (C) Data from two experiments with five mice. (D and E) Histopathology of lung sections stained with HE and PAS. Five sections from each of three mice in each group were evaluated in a blinded fashion according to the scoring system described in Materials and methods. (F and G) Relative frequency of CD4 and CD8 cells in lung parenchyma after aerosol exposure and blockade of TL1A for different periods of time. Single-cell suspensions were analyzed by flow cytometry gating on the lymphocyte gate. (H–J) RNA was isolated from whole lungs and analyzed by real-time PCR as in Fig. 3. Error bars represent the mean ± the SEM.

Antibody blockade of TL1A inhibits lung inflammation of antigen-primed mice even after airway antigen reexposure

The effect of TNFR25 signals on IL-13 secretion by NKT cells (Fig. 1 B) suggested that TNFR25 may be an important costimulus for IL-13 production in the lung. Invariant NKT cells producing IL-13 have previously been shown to be essential for the induction of lung inflammation and airway hyperreactivity in the murine ovalbumin model for allergic, atopic lung inflammation (23). We therefore tested whether blockade of TNFR25 signals in vivo would have effects on lung inflammation in the classical ovalbumin model. Blockade of TNFR25 signals in vivo can be achieved by blocking the cognate ligand TL1A with an antagonistic TL1A antibody (L4G6) or by genetic means, generating dominant-negative (DN) mutants of TNFR25.

To test TNFR25 blockade with anti-TL1A, mice were immunized twice with ovalbumin in alum on day 0 and 5, and were airway challenged on day 12 with aerosolized ovalbumin. 1 d before airway challenge, and for the next 3 d, 50 µg anti-TL1A-IgG L4G6 or control hamster IgG was administered i.p., and the mice were analyzed the next day. L4G6 administered in this way at the time of aerosol challenge strongly inhibited lung inflammation, as indicated by decreased cellular exudation into BALF (Fig. 3 A) and by reduced mucus production as detected in tissue section by periodic acid-Schiff (PAS) staining (Fig. 3 B). In anti-TL1A (L4G6)–treated mice, IL-13 and -5 secretion by bronchial draining lymph node cells upon restimulation with ovalbumin in vitro was significantly inhibited compared with

IgG-treated control mice (Fig. 3 C). IL-4 was undetectable in control and anti-TL1A–treated mice.

Lung inflammation in the ovalbumin model is known to be associated with Th2 cytokine production in bronchial lymph nodes. Using Taqman PCR assays, we found IL-13 mRNA to be up-regulated by >100-fold and IL-5 mRNA to a lower degree in lung tissues of ovalbumin-aerosolized mice (Fig. 3 D). Anti-TL1A administration started 1 d before aerosol blocked the up-regulation of Th2 cytokine mRNA (Fig. 3 E).

To determine whether TL1A blockade of lung inflammation was effective even when started after airway antigen reexposure, we compared the effect of TL1A blockade on inflammation by beginning antibody administration from 24 h before to 72 h after ovalbumin aerosol exposure (Fig. 4). Anti-TL1A fully blocked lung inflammation when administration started at −24, 0, and +24 h relative to airway antigen exposure. Significant inhibition of lung inflammation by anti-TL1A was still observed, even when the antibody was administered 48 and 72 h after aerosol exposure. The 72-h time point allowed for only 4 h of in vivo action of anti-TL1A, but was still able to significantly reduce eosinophil infiltration by ∼50%, suggesting potential therapeutic activity (Fig. 4 C). The rapid reduction of eosinophils in BALF within 4 h after anti-TL1A administration suggests that anti-TL1A disrupts an ongoing inflammatory reaction recruiting eosinophils and/or supporting their maintenance. Histopathology by hematoxylin and eosin (HE) and PAS staining of

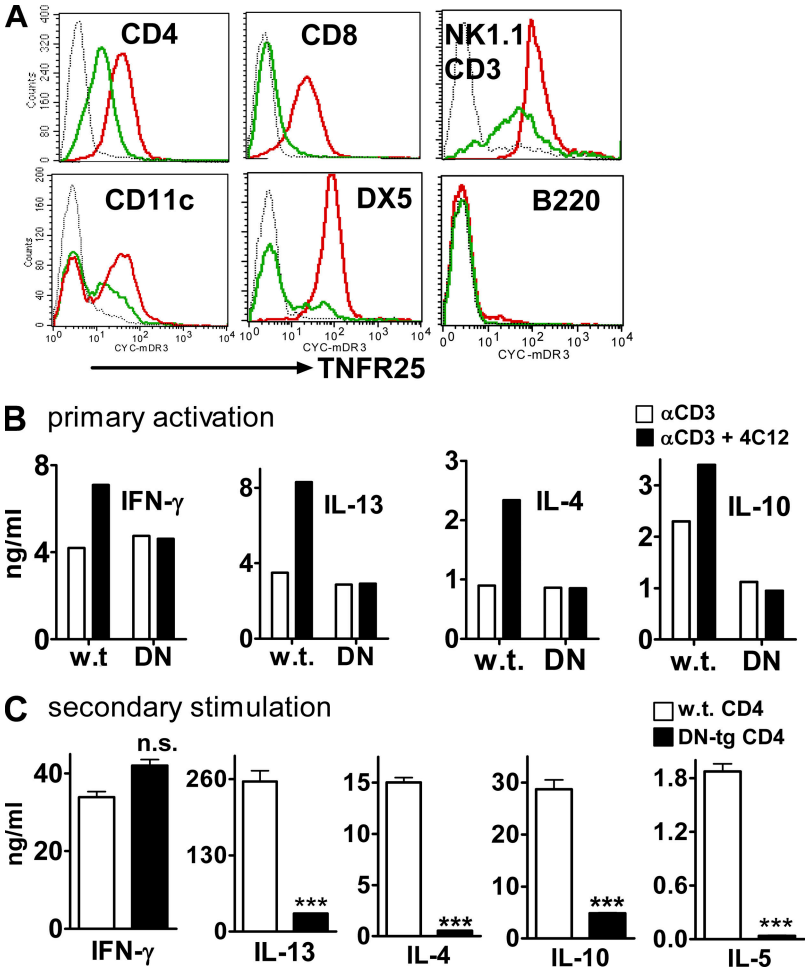

Figure 5. DN TNFR25 transgene blocks TNFR25 signaling and interferes with Th2 cytokine production upon secondary stimulation. (A) Expression of DN-TNFR25-tg on lymph node cells. Lymph node cells were gated on CD4, CD8, CD11c, B220, DX5, or NK1.1/CD3; TNFR25 expression is displayed in the histogram. Black curves, isotype controls; red curves, DN TNFR25-tg lymph node cells; green curves, nontransgenic lymph node cells from littermates; all cells are in resting, nonactivated state. (B) DN TNFR25-tg blocks cytokine co-stimulation by agonistic anti-TNFR25 (4C12). Purified WT and DN TNFR25-tg (DN) CD4 cells were stimulated for 3 d with anti-CD3 with or without the agonistic anti-TNFR25 antibody 4C12 (5 µg/ml). The supernatants were analyzed for cytokines by ELISA. (C) DN TNFR25-tg CD4 T cells do not exert Th2 cytokine production in secondary activation. WT and DN TNFR25-tg CD4 T cells were purified by negative selection and activated with 2 µg/ml immobilized anti-CD3 and 1 µg/ml soluble anti-CD28 for 3 d under Th cell neutral conditions (no cytokines were added). Cells were harvested, washed, replated, and restimulated with 1 µg/ml immobilized anti-CD3 for 2 d. The supernatants were collected for cytokine ELISA assay. All experiments were performed more than three times with reproducible results. Error bars represent the mean ± the SEM. ***, $P < 0.001$.

the lung revealed decreased numbers of infiltrating cells around blood vessels and bronchioli and decreasing mucus already within 4 h of TL1A blockade (Fig. 4, D and E). The relative frequency of CD4 and CD8 cells detected in the lymphoid gate in the lung parenchyma is slightly increased after 4 h TL1A blockade and decreases upon longer L4G6 presence (Fig. 4, F and G). The early, relative increase in the frequency of CD4 and CD8 cells after only 4 h of TL1A blockade may be caused by the rapid loss of eosinophils that represent a large proportion of infiltrating cells. The frequency of NKT cells varied in the lymphoid gate in all samples without a clear tendency of change (unpublished data). Anti-TL1A, present for 4 and 24 h, suppressed IL-4, -5, and -13 mRNA but did not affect IFN-γ mRNA (Fig. 4, H and J). The data suggest that TL1A blockade has immediate inhibitory effects on the effector phase of lung inflammation without early effects on lymphoid cell populations.

Our data support the concept that TL1A is needed for the engagement of TNFR25 in vivo, and that continuous TNFR25 signals contribute to or are critical for Th2 and IL-13 production and lung inflammation. To further test and independently confirm that blockade of TNFR25 signals inhibit susceptibility to allergic lung inflammation, we developed a genetic model for TNFR25 blockade on T cells and NKT cells by creating a DN TNFR25 transgene that is expressed on T cells.

DN TNFR25 transgene blocks TNFR25 signaling and lung inflammation

To confirm the role of TNFR25 in the induction of lung inflammation by independent, genetic methods, we generated a DN mutant of TNFR25, DN TNFR25, and expressed the construct as transgene under the CD2 promoter and enhancer on T cells and NKT cells. The DN TNFR25-transgene is lacking the entire intracellular signaling domain, but is identical to full-length TNFR25 in its transmembrane and extracellular domain. Trimerization of DN TNFR25 with endogenous TNFR25 is expected to extinguish TNFR25 signaling. Transgenic DN TNFR25 was expressed constitutively on resting T cells, NKT, NK, and a subpopulation of $CD11c^+$ cells (Fig. 5 A, red) as determined by flow cytometry. The expression of endogenous TNFR25 on resting cells of nontransgenic litter mates is also shown (in green in Fig. 5 A). The fluorescence intensity indicates that the DN TNFR25 expression level is higher than endogenous TNFR25 and may be sufficient to act as a DN mutant. DN TNFR25-transgene (tg) mice appear healthy, and they have normal white cell counts in thymus, spleen, and lymph nodes. The number and phenotype of $CD4^+$ and $CD8^+$ T cells, B cells, $CD11c^+$ cells, NK, and NKT cells is normal.

To assure that the level of overexpression of DN TNFR25 silenced the activity of endogenous TNFR25, several experiments were performed. Primary anti-CD3 activation of naive WT and DN-TNFR25-tg CD4 cells stimulates Th1 and Th2 cytokine secretion equally (Fig. 5 B). In WT CD4 cells, cytokine production is co-stimulated by TNFR25 signals elicited with the agonistic anti-TNFR25 antibody 4C12. This co-stimulation by 4C12 is not observed in DN TNFR25-tg CD4 cells (Fig. 5 B), indicating that the DN TNFR25 transgene product blocks the function of endogenous TNFR25. Similarly, TNFR25 signals co-stimulated proliferation of activated WT CD4 cells, and this co-stimulation is not observed in DN TNFR25-tg CD4 cells (unpublished data)

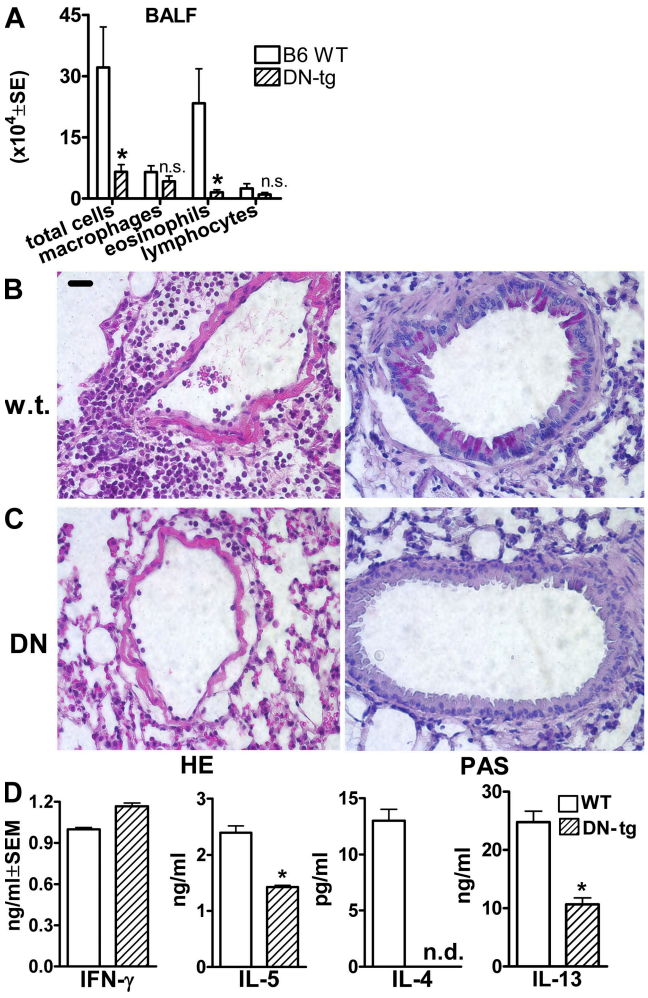

Figure 6. Genetic blockade of TNFR25 abolishes lung inflammation. (A) Diminished cellular exudation in BALF in DN TNFR25-tg mice. Mice were primed and aerosol challenged with ovalbumin according to our standard protocol. $n = 5$. *, $P < 0.05$. (B and C) Suppression of lung inflammation in DN TNFR25-tg mice after immunization and airway challenge. Lung inflammation was induced by ovalbumin immunization, and subsequent aerosol exposure as described. (B) Wild-type B6. (C) DN TNFR25-tg B6 mice. Note absence of perivascular infiltrates in DN TNFR25-tg mice after antigen aerosol exposure and absence of mucus over production and goblet cell hyperplasia in DN TNFR25-tg mice. (D) Suppression of Th2, but not Th1, cytokine production in DN TNFR25-tg bronchial lymph nodes from aerosol-challenged mice. Bronchial lymph nodes were harvested 3 d after aerosol challenge, and lymph node cells were prepared and restimulated with 100 µg/ml ovalbumin for 4 d. Supernatants were then analyzed for cytokine production by ELISA. This figure is the representative of two independent experiments ($n = 4$). n.d., not detected. *, $P < 0.05$. Error bars represent the mean ± the SEM.

indicating that endogenous TNFR25 is silenced by the DN mutant TNFR25.

It is well established that cytokine production by CD4 cells is greatly amplified upon secondary stimulation. Importantly, DN TNFR25-tg CD4 cells upon secondary activation do not support up-regulated production of Th2 cytokines, while allowing amplified IFN-γ production (Fig. 5 C), suggesting that TNFR25 signals are required for amplified Th2 cytokine secretion. The data suggest that TNFR25 may have a dual effect in lung inflammation by co-stimulating IL-13 secretion by NKT cells and by amplifying Th2 cytokine production in ovalbumin-restimulated CD4 T cells in the lung. Based on these observations, we tested whether DN-TNFR25-tg mice showed an altered response to the induction of lung inflammation in our ovalbumin model.

Ovalbumin-primed, DN TNFR25-tg mice upon airway challenge with ovalbumin exhibited significantly diminished eosinophilic infiltration in BALF (Fig. 6 A), absent lung inflammation and mucus production by histopathology (Fig. 6, B and C), and diminished ovalbumin-specific IgE production (unpublished data) in serum. In vitro, ovalbumin restimulation of bronchial draining lymph node cells harvested from primed and airway-challenged DN TNFR25-tg mice mediated diminished Th2 cytokine production but normal IFN-γ production (Fig. 6 D). These data support the concept that TNFR25 signals play a critical role in pulmonary immune responses and lung inflammation by triggering IL-13 production by NKT cells and amplifying Th2 cytokine production by Th2-polarized CD4 cells. To directly test the role of NKT cells in vivo, adoptive transfer experiments with DN-TNFR25-tg NKT cells were performed.

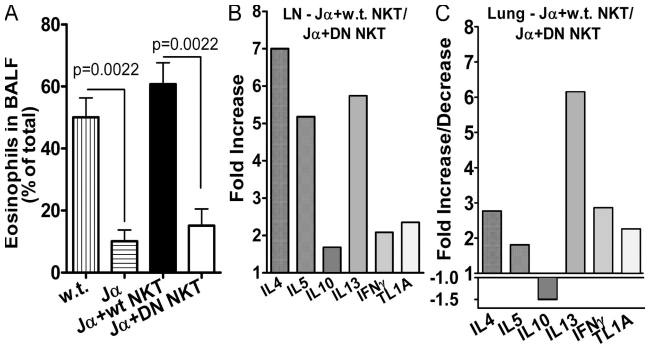

Figure 7. TNFR25 signals on NKT cells are required for induction of lung inflammation. NKT-deficient Jα18 KO mice (28) were primed with ovalbumin and alum as in our standard protocol in Materials and methods. On day 11, the mice received 3.1 million purified NK/NKT cells containing 1 million WT NKT cells or DN TNFR25-tg NKT cells (DN NKT) or PBS by i.v. adoptive transfer, as indicated. The mice were exposed to ovalbumin aerosol on day 12 and analyzed on day 15. WT mice and Jα18 KO mice receiving WT NKT cells by adoptive transfer served as positive controls for induction of lung inflammation. Jα18 KO mice, immunized and ovalbumin aerosolized without adoptive cell transfer, served as negative controls. The data of three independent experiments and two mice in each group are shown. (A) Eosinophils in BALF. Error bars represent the mean ± the SEM. (B and C) Cytokine and TL1A mRNA expression in bronchial lymph nodes (LN; B) and lung parenchyma (C) determined by real time Taqman PCR. The fold increase or decrease of mRNA in Jα18 KO mice (Jα) adoptively transferred with WT NKT cells over mice adoptively transferred with DN TNFR25-tg NKT (DN NKT) cells is plotted.

Adoptive transfer of DN TNFR25-tg NKT cells does not restore lung inflammation in NKT-deficient mice.

To further assess the role of TNFR25 in NKT cell function in lung inflammation, we made use of the fact that NKT-deficient mice (Jα18 KO) (27) are resistant to induction of lung inflammation in the ovalbumin model (21, 23, 24). Adoptive transfer of WT NKT cells to NKT-deficient, Jα18 KO mice restores lung inflammation and airway hyperreactivity in the ovalbumin model. Akbari et al. (23) also showed that adoptive transfer of NKT cells from IL-13-deficient mice did not restore lung inflammation in Jα18 KO mice, demonstrating the importance of IL-13 production by NKT cells in the induction of lung inflammation. Because our data indicated that IL-13 production by NKT cells is co-stimulated by TNFR25, we hypothesized that adoptive transfer of DN TNFR25-tg NKT cells likewise would not be able restore lung inflammation in NKT-deficient mice.

We purified NK/NKT cells by positive selection from the spleens of 10 mice, and we adoptively transferred i.v. 1 million DN TNFR25-tg NKT cells, corresponding to 3 million NK/NKT cells, into ovalbumin-primed, NKT-deficient (Jα18 KO) mice (27). Adoptive transfer of 1 million WT NKT cells served as controls. On the day after adoptive transfer the mice were subjected to aerosolized ovalbumin. 3 d later, lung inflammation was measured by the degree of eosinophil exudation into the BALF (Fig. 7 A) and by cytokine mRNA expression in lung parenchyma and bronchial draining lymph nodes (Fig. 7, B and C). Although adoptively transferred WT NKT cells restored lung inflammation and BALF eosinophilia upon airway antigen challenge, the same number of DN TNFR25-tg NKT cells was unable to do so (Fig. 7). The diminished BALF eosinophilia (Fig. 7 A) observed in DN TNFR25-tg NKT cell-transferred mice was associated with diminished Th2 cytokine mRNA induction in lung tissues and in bronchial draining lymph nodes (Fig. 7, B and C). In lung tissue, IL-13 mRNA was markedly reduced, whereas in bronchial lymph nodes, IL-4 and -5 mRNA were also strongly affected by the absence of functional TNFR25 on NKT cells. In addition, TL1A mRNA was twofold higher in mice receiving WT NKT cells, suggesting positive feedback amplification of TL1A expression by TNFR25-induced Th2 cytokine production. The data demonstrate that TNFR25 signals in NKT cells are necessary and sufficient for triggering lung inflammation during airway antigen exposure of sensitized mice even under conditions when normal TNFR25-signals can be elicited on CD4 cells.

DISCUSSION

The signature cytokine of asthma is IL-13 (30), and NKT cells appear to be an important early source of IL-13 production in the lung (23). Our study indicates that an essential

trigger for IL-13 secretion by NKT cells and Th2 cytokine production in the lung is TNFR25. This conclusion is supported by the evidence that TNFR25 in vitro acts as a co-stimulus for IL-13 secretion by NKT, together with the activation of the invariant TCR by glycosphingolipid or low concentration of anti-CD3. TNFR25 signals also increase the number of IL-13–producing NKT cells, by inducing IL-13–producing cells at intermediate TCR stimulation. The effect of TNFR25 co-stimulation on NKT cells appears to be specific for IL-13, and to a lesser extent IL-4, whereas IFN-γ secretion by NKT cells is not co-stimulated by TNFR25.

The importance of TNFR25 signals in lung inflammation is further supported by in vivo blocking experiments using an antagonistic anti-TL1A antibody and by genetic blockade of TNFR25 signals with a DN mutant TNFR25 transgene. In vivo, blockade of TNFR25 results in inhibition of all signs of lung inflammation, including down-regulation of IL-4, -5, and -13 mRNA in lung parenchyma and bronchial lymph nodes, diminished Th2 cytokine production after ex vivo antigen restimulation of draining bronchial lymph nodes, diminished BALF eosinophilia, and diminished mucus production. The potent effect of anti-TL1A on BALF eosinophilia is noteworthy. 4 h of TL1A blockade, from 72 to 76 h after airway antigen exposure, was reproducibly able to significantly reduce BALF eosinophilia by ∼50%. It is known that eosinophil-accumulation peaks on day 3 after airway antigen exposure. In culture, eosinophils are short lived unless IL-5 is added, which supports eosinophil survival (31–33). Thus, TL1A may be needed for stimulation of TNFR25 signals for continued IL-5 and -13 production, thereby sustaining continued survival and/or migration of eosinophils into BALF. In support of this hypothesis, we found that in vitro continuous anti-CD3 stimulation of CD4 cells maintains high levels of TL1A expression for >4 d. Withdrawal of TCR stimulation results in TL1A down-regulation within 24 h (unpublished data). Alternatively, eosinophils may express TNFR25, which has not been studied so far, and it may act as a direct survival factor. Finally, it has been reported that TL1A is expressed by certain endothelial cells (11), and thus may be involved in eosinophil migration and extravasation.

The data also indicate that TNFR25 co-stimulation during secondary activation of CD4 cells greatly amplifies Th2 cytokine production. According to recent reports, Th2 polarization involves gain of Th2 effector function, followed by ITK-mediated signals that are required for the exertion (amplification) of Th2 effector function upon TCR restimulation (34, 35). The upstream signals leading to ITK activation have not been identified. It is possible that TNFR25 signals play a role in this sequence; a hypothesis is currently under investigation. In support, we have found that functional TNFR25 transgenes on T cells result in spontaneous Th2 production of CD4 cells upon primary activation (unpublished data). The strong effects of TNFR25 blockade on lung inflammation, therefore, appear to be caused by the dual action of TNFR25, first at the level of NKT cells and second at the level of polarized CD4 T cells.

We were able to further support the role of TNFR25 on NKT cells through adoptive transfer experiments of NKT cells into NKT-deficient mice. NKT-deficient mice are resistant to lung inflammation, but can be rendered susceptible by adoptive transfer of WT NKT cells before airway antigen exposure. On the other hand, adoptive transfer of IL-13–deficient NKT cells is unable to restore lung inflammation in NKT-deficient mice (23); similarly, we show that adoptive transfer of DN TNFR25-tg NKT cells is unable to restore lung inflammation. This finding is consistent with the interpretation that TNFR25 signals in vivo are required to trigger IL-13 secretion by NKT cells in the ovalbumin model of lung inflammation. Absence of either IL-13 or TNFR25 signals triggering IL-13 release by NKT cells results in aborted lung inflammation upon airway antigen exposure of primed mice.

TNFR25 is triggered by ligation to TL1A, as indicated by the antibody blockade using antagonistic anti-TL1A. TL1A is not detectable by PCR in the normal lung, but is up-regulated on the mRNA level as measured by Taqman assays in bronchial lymph nodes and lung tissue during lung inflammation. CD4 and CD8 T cells and APC can express TL1A upon activation. It is known that TL1A can be released as soluble ligand after proteolytic cleavage. Therefore, it is possible that TL1A may act as soluble mediator or as cell-bound ligand to trigger TNFR25 on NKT and T cells.

Regardless of the specific details of TL1A expression as soluble or cell-bound molecule, our data add an important molecular component (TNFR25/TL1A) to our understanding of the pathogenesis of lung inflammation, a cardinal feature of asthma. Our data support and extend previous findings of the importance of NKT cells and IL-13 in lung inflammation and in airway hyperreactivity. We present evidence that TNFR25 is the essential trigger for IL-13 release by NKT cells and for amplification of the Th2 response by Th2-polarized CD4 cells. These functions distinguish TNFR25 from Ox40, which supports survival of Th2-polarized CD4 T cell (36, 37). In contrast, TNFR25 specifically promotes the exertion of effector function of Th2-polarized cells, in addition to triggering IL-13 production by NKT cells. Whether Ox40 has any effects on NKT cells is not known.

Attenuation of lung inflammation is an important goal for the treatment of atopic asthma, which is inexorably rising in incidence and severity. Our data show that lung inflammation can be inhibited by TNFR25 blockers in mice that have already been primed and sensitized. Importantly, TL1A blockade even 72 h after airway antigen reexposure of sensitized mice, for 4 h before analysis, attenuates lung inflammation. This finding, and the observation that TNFR25 appears to be very far upstream in the inflammatory sequence, may make it a valuable target for drug development for the treatment of asthma patients.

MATERIALS AND METHODS

Media and reagents. Cells were cultured in Iscove's Modified Dulbecco's Minimal Essential Medium (Invitrogen) supplemented with 10% heat-inactivated FBS (Invitrogen), 10 μg/ml gentamycin (Invitrogen), and

50 μM β-mercaptoethanol (Bio-Rad Laboratories). Monoclonal anti–mouse and anti–human CD3 were purified from cultured supernatants of the 2C11 (American Type Culture Collection). Monoclonal anti–mouse CD28 was purchased from eBioscience. ConA, PHA, and LPS were purchased from Sigma-Aldrich. Recombinant murine IL-2 and -15 was obtained from BioSource International). PMA, ionomycin, H7, and cycloheximide were purchased from Calbiochem.

Directly conjugated monoclonal antibodies, including FITC-CD4, Cychrome-CD4, PE-CD8α, Cychrome-CD8α, FITC-B220, PE-B220, FITC-CD25, PE-CD11c, PE-DX5, FITC-CD3, PE-NK1.1, PE-Annexin V, and 7-amino actinomycin were purchased from BD Biosciences. Hamster IgG control was purchased from eBioscience.

Generation of monoclonal antibodies against mTNFR25 and mTL1A. Armenian hamsters were immunized intraperitoneally 3 times biweekly with 50 μg of mTNFR25-Ig or mTL1A-MBP (maltose binding protein) in Freund's adjuvant. 3 d before the fusion, hamsters were boosted with 50 μg of the respective proteins i.v. Hamster splenocytes were fused with the murine myeloma SP20 with PEG, and then plated in methylcellulose-based medium for 2 wk using ClonaCell-HY kit (StemCell Technologies). 1,000 colonies were picked and analyzed by ELISA in plates coated with the immunizing fusion protein or control protein-Ig fusion protein. Supernatants from positive clones were tested for the ability to detect TNFR25 or TL1A in transfected cells by flow cytometry and Western blotting. Antibodies were purified from a Nutridoma-SP (Roche) supernatant on a protein G column, dialyzed into PBS, and filter sterilized.

Flow cytometric analysis for the expression of TNFR25 and TL1A. Single-cell suspensions were prepared from lymphoid organs indicated in the individual experiment. Before staining, cells were treated with purified anti–mouse CD16/CD32 (Fc-γIII/II receptor; BD) and purified human IgG (Jackson ImmunoResearch Laboratories) to block nonspecific binding to FcRs. Cells were stained with Armenian hamster anti–mouse TNFR25 or anti–mouse TL1A for 30 min at 4°C. Cells were washed in FACS buffer (PBS containing 0.5% BSA and 2 mM EDTA) and stained with biotin-labeled goat anti–Armenian hamster IgG (Jackson ImmunoResearch Laboratories) for 30 min at 4°C. Cells were washed and stained with Streptavidin-PE or Streptavidin-Cychrome (BD Biosciences) for 30 min at 4°C. Cells were washed and stained with directly conjugated cell surface markers for distinct cell populations. Samples were analyzed using a FACS LSR instrument (Becton Dickinson) and CellQuest software.

Nuclear extract preparation and electrophoretic mobility shift assays for NF-κB activation. 10^7 EL4-TNFR25 cells were treated with soluble or membrane-bound TL1A or with the TNFR25 agonistic antibody 4C12, as indicated in the figure legends, and then collected by centrifugation at 800 *g* for 5 min. Nuclear extracts were isolated using a minipreparation protocol and subjected to EMSA as previously described (38). Nuclear extracts (6 μg) were incubated at room temperature for 20 min with a ^{32}P-labeled high-affinity κB probe, followed by resolving the DNA–protein complexes on native 5% polyacrylamide gels.

Generation of transgenic mice. A murine DN mutant of TNFR25 lacking the intracellular domain (DN TNFR25, aa 1–234) was cloned under the human CD2 promoter and local control region (gift from A. Singer, National Institutes of Health) using the restriction endonuclease sites EcoRI and SalI. Microinjections of DNA into the fertilized eggs were performed by the transgenic facility at the University of Miami Miller School of Medicine. Potential founders were screened by PCR of DNA from tail biopsies. The primer pair was located upstream and downstream of the cloning sites. The upstream primer is 5′-CGCTCTTGCTCTCTGTGTATG-3′ and the downstream primer is 5′-CTGCCAGCCCTCTTCCATC-3′. Transgenic mice were bred into the C57BL/6J background by serially mating hemizygous transgenic animals with WT C57BL/6J (The Jackson Laboratory). All mice were used at 6–12 wk of age and were maintained in pathogen-free facilities. The University of Miami Animal Care and Use Committee approved all animal use procedures.

T cell proliferation assay. Splenocytes were plated in triplicate at 1×10^5 cells/well in 96-well flat-bottom plates. Cells were activated with 2 μg/ml immobilized anti-CD3 with or without 1 μg/ml soluble anti-CD28, or with 5 μg/ml ConA or 10 ng/ml PMA and 400 ng/ml ionomycin. For T cell proliferation, purified CD4 T cells at 1×10^5 cells/well or CD8 T cells at 5×10^4 cells/well were stimulated with 2 μg/ml coated anti-CD3 and 1 μg/ml soluble anti-CD28. Recombinant mIL-2 was added to the culture at 1,000 U/ml in the indicated experiments. Cells were cultured for 72 h and pulsed for the last 6 h of incubation, with 1 μCi/well of [^{3}H]thymidine (PerkinElmer), and thymidine incorporation was quantitated using a scintillation counter.

Murine CD4 or CD8 T cells were purified from splenocytes and/or lymph nodes by negative selection using the SpinSep kit (StemCell Technology Inc.) according to the manufacturer's protocol. The purity was routinely ~90–96%, as examined by FACS analysis.

Immunization protocol for the murine model of allergic asthma. DN TNFR25-tg mice generated as described above and backcrossed at least seven generations into the C57BL/6J background were compared with WT C57BL/6J mice purchased from the National Cancer Institute. Mice were sensitized by i.p. injection of 66 μg ovalbumin (crystallized chicken egg albumin, grade V; Sigma-Aldrich) absorbed to 6.6 mg aluminum potassium sulfate (alum; Sigma-Aldrich) in 200 μl PBS on day 0. On day 5, mice were boosted intraperitoneally with the same dose of ovalbumin in alum. On day 12, mice were aerosol challenged with 0.5% ovalbumin in PBS for 1 h using an Ultrasonic Nebulizer (MABIS Healthcare, Inc.). Mice were assessed for allergic inflammation of the lungs 1–3 d (on day 13 to 15) after the aerosol exposure. Mice were killed by inhalation of CO_2. After cannulation of the trachea, the lung was lavaged 4 times with 1 ml of PBS. Cells recovered from the BAL fluid were counted and used for cytospin preparations (≤50,000 cells/slide). More than 200 cells were counted for each cytospin slide stained with Wright-Giemsa stain (Sigma-Aldrich) to determine differential cell counts for macrophages, eosinophils, lymphocytes, and neutrophils.

Lung histology. Lungs were removed from mice after the bronchial lavage procedure and fixed in 10% neutral buffered formalin. Samples were submitted to the Histopathology Core of the Sylvester Cancer Center at the University of Miami Miller School of Medicine, where specimens were embedded, sectioned, and stained with HE. Sections were also stained with PAS to determine mucus production. Five lung sections of each experimental animal were evaluated. Slides were coded and scored in a blinded fashion. The following scoring system was used for HE-stained sections (39). A value from 0 to 3 per criterium was adjudged to each tissue section scored. Two criteria were scored to document the pulmonary inflammation: peribronchial inflammation and perivascular inflammation. A value of 0 was adjudged when no inflammation was detectable, a value of 1 for occasional cuffing with inflammatory cells, a value of 2 when most bronchi or vessels were surrounded by a thin layer (1–5 cells) of inflammatory cells, and a value of 3 when most bronchi or vessels were surrounded by a thick layer (>5 cells) of inflammatory cells. For PAS-stained sections, the scoring system according to Roh et al. (40) was used. Section analysis for PAS staining was also performed in a blinded fashion using a quantitative scoring system (0–4), where 0 represented no epithelial staining, 1 represented slight epithelial staining, 2 represented moderate epithelial staining, 3 represented heavy epithelial staining, and 4 represented massive epithelial staining.

ELISA for serum total IgE and ovalbumin-specific IgE. Mice were bled before sensitization (day 0), 3 d after aerosol challenge (day 15), and, in some experiments, 1 d before aerosol challenge (day 11). The total IgE level was quantitated by ELISA according to the manufacturer's protocol (BD Biosciences). Ovalbumin-specific IgE was determined in Sandwich ELISA by first coating the plate with 0.01% ovalbumin in PBS, followed by loading diluted serum samples and the secondary biotin–labeled anti-IgE antibody (BD Biosciences).

In vitro restimulation of bronchial lymph node cells and cytokine production. 3 d after aerosol challenge, bronchial lymph nodes were harvested, and single-cell suspensions were prepared. Cells were seeded into round-bottom 96-well plates at 1×10^6 cells/well and cultured with 100 μg/ml ovalbumin for 4 d. Supernatants were collected for cytokine ELISA assays as described.

Cytokine mRNA levels were measured by quantitative Taqman PCR. Before the homogenizing procedure, lungs and lymph nodes were suspended in 3 and 1.5 ml, respectively, of ice cold lysing buffer RLT (RNeasy mini kit; QIAGEN). Homogenization was performed in a 50-ml conical centrifuge tube, using a 12-mm generator attached to a standalone Polytron PCU-2 (Brinkman) homogenizer unit. Tubes were maintained on ice throughout the homogenization process. Subsequently, 0.7 ml of homogenized tissues was further homogenized using QIAshredder Mini Spin columns (QIAGEN). Extraction of RNA was performed using the RNeasy mini kit following the manufacturer's recommendations for purification of total RNA from animal tissue. An on-column DNase digestion was also performed using RNase-Free DNase (QIAGEN). The quality of RNA was assessed by capillary chromatography and quantitated by spectrophotometry. Reverse transcription of 1 μg of RNA per sample, was performed using the Quantitect reverse transcription kit (QIAGEN), following recommendations from the manufacturer. Real-Time PCR was performed in a 7300 Real-Time PCR system (Applied Biosystems) using dual-labeled fluorogenic probe-based Taqman technology. Gene expression assays (Applied Biosystems) for IL-4 (Mm00445259_m1), IL-5 (Mm00439646_m1), IL-10 (Mm00439616_m1), IL-13 (Mm00434204_m1), IFN-γ (Mm00801778_m1), and TL1-A(Mm00770031_m1) were performed and normalized to GAPDH (part number 4352932E; Applied Biosystems) gene expression, and fold differences calculated using the ΔCt method.

Cytotoxicity assay. Soluble TL1A supernatants harvested from P815-TL1A transfected cells were added to ^{51}Cr-labeled P815-TNFR25 transfected target cells. To test for TL1A blocking activity, different anti-TL1A monoclonal antibodies were added into the culture and Cr release determined in triplicate samples after 4 h incubation. Spontaneous release was calculated from the wells that contained only ^{51}Cr-labeled target cells. 100% release (positive control) was calculated from the wells that contained ^{51}Cr-labeled target cells and 1% SDS.

Blocking of lung inflammation by antagonistic anti-mTL1A antibody. Mice were sensitized intraperitoneally with ovalbumin in alum on day 0 and day 5, followed by aerosol challenge with 0.5% ovalbumin in PBS for 1 h on day 12. Mice were given antagonistic L4G6 or nonblocking L3A10 anti-Tl1A or an equivalent amount of the control hamster IgG (Jackson ImmunoResearch Laboratories) by intraperitoneal injection of 50 μg/mouse each day from day 11 to 14 or as indicated in the graphs. Allergic lung inflammation was evaluated on day 13–15.

Preparation of NKT cells for in vitro evaluation and adoptive transfer. Jα18 KO mice (27) were a gift from M. Lotze (University of Pittsburgh, Pittsburgh, PA) with permission from M. Taniguchi (Ciba University, Ciba, Japan). NKT cells from WT and DN TNFR25-tg mice were enriched from pooled spleen cells from 10 mice by positive selection using the EasySep mouse Pan-NK-Positive Selection kit (StemCell Technologies) according to the manufacturer's instructions. The ratio of NK to NKT cells in the enriched population was 65:35.3 million cells containing 1 million WT or DN TNFR25-tg NKT cells were adoptively transferred i.v. through the tail vein to ovalbumin-primed mice, and the mice were aerosolized on the next day and analyzed 2 d later.

NK/NKT cells were isolated in the same way for in vitro analysis of cytokine co-stimulation by agonistic anti-TNFR25. 200,000 cells were incubated for 48 h in flat bottom, 96-well microtiter plates in triplicate in the presence of 10 ng/ml IL-15 with 0, 20, 100, or 500 ng/ml of the glycosphingolipid OCH. The lipid OCH is identical to α-galactosylceramide except for a shorter sphingosine chain (41). Co-stimulation was achieved with 5 μg/ml agonistic anti-TNFR25 antibody 4C12. After 48 h, supernatants were harvested and analyzed by ELISA for IL-13, IL-4, and IFN-γ.

For intracellular cytokine staining, enriched NK/NKT cells were cultured at 2×10^5 cells/well in a 96-well, flat-bottom plates for 72 h in the presence of plate-bound anti-CD3, as indicated in the figures with or without anti-TNFR25 at 5 μg/ml. Activated cells were harvested after 67 h, washed twice in media, and counted. Cells were replated at 2×10^5 cells per well in 96 flat-bottom well plates for 5 h in the presence of PMA (at 10 nM) and ionomycin (at 0.25 μM) and Monensin (at 2 μM). After the 5 h, cells were harvested (not counted) and transferred directly into staining tubes (3–4 wells worth of cells per tube = 8×10^5 cells). Staining began with cell surface stain with CD3 PerCP and NK1.1 FITC. Cells were then fixed and permeabilized at room temperature, followed by an incubation with the specific intracellular cytokine stain (IL-13 Alexa Fluor 647 and IFN-γ Pacific Blue) or isotype control. For the IL-13 staining control, 1 μg rIL-13 was used to preblock anti–IL-13, which then proceeded to stain as with the unblocked IL-13 antibody. All antibodies and reagents used for the intracellular cytokine stain were purchased from eBioscience, except for the CD3 PerCP which was purchased from BD Biosciences. Data were acquired on BD LSRII with BD DIVA software. Files were then converted and analyzed using Cell Quest.

Statistical analyses. Statistical analyses using a two-tailed Student's *t* test were performed with GraphPad Prism Software. $P < 0.05$ is considered significant. Data in the text are presented as the mean ± the SEM.

We gratefully acknowledge the outstanding assistance of Patricia Guevara and Jahir Ramos.

This work was supported by USPHS grants CA 39201 and AI 061807.

The authors have no conflicting financial interests.

Submitted: 29 November 2007
Accepted: 11 March 2008

REFERENCES

1. Chinnaiyan, A.M., K. O'Rourke, G.L. Yu, R.H. Lyons, M. Garg, D.R. Duan, L. Xing, R. Gentz, J. Ni, and V.M. Dixit. 1996. Signal transduction by DR3, a death domain-containing receptor related to TNFR-1 and CD95. *Science*. 274:990–992.
2. Kitson, J., T. Raven, Y.P. Jiang, D.V. Goeddel, K.M. Giles, K.T. Pun, C.J. Grinham, R. Brown, and S.N. Farrow. 1996. A death-domain-containing receptor that mediates apoptosis. *Nature*. 384:372–375.
3. Screaton, G.R., X.N. Xu, A.L. Olsen, A.E. Cowper, R. Tan, A.J. McMichael, and J.I. Bell. 1997. LARD: a new lymphoid-specific death domain containing receptor regulated by alternative pre-mRNA splicing. *Proc. Natl. Acad. Sci. USA*. 94:4615–4619.
4. Bodmer, J.L., K. Burns, P. Schneider, K. Hofmann, V. Steiner, M. Thome, T. Bornand, M. Hahne, M. Schroter, K. Becker, et al. 1997. TRAMP, a novel apoptosis-mediating receptor with sequence homology to tumor necrosis factor receptor 1 and Fas(Apo-1/CD95). *Immunity*. 6:79–88.
5. Marsters, S.A., J.P. Sheridan, C.J. Donahue, R.M. Pitti, C.L. Gray, A.D. Goddard, K.D. Bauer, and A. Ashkenazi. 1996. Apo-3, a new member of the tumor necrosis factor receptor family, contains a death domain and activates apoptosis and NF-kappa B. *Curr. Biol*. 6:1669–1676.
6. Tan, K.B., J. Harrop, M. Reddy, P. Young, J. Terrett, J. Emery, G. Moore, and A. Truneh. 1997. Characterization of a novel TNF-like ligand and recently described TNF ligand and TNF receptor superfamily genes and their constitutive and inducible expression in hematopoietic and non-hematopoietic cells. *Gene*. 204:35–46.
7. Boldin, M.P., E.E. Varfolomeev, Z. Pancer, I.L. Mett, J.H. Camonis, and D. Wallach. 1995. A novel protein that interacts with the death domain of Fas/APO1 contains a sequence motif related to the death domain. *J. Biol. Chem*. 270:7795–7798.
8. Chinnaiyan, A.M., K. O'Rourke, M. Tewari, and V.M. Dixit. 1995. FADD, a novel death domain-containing protein, interacts with the death domain of Fas and initiates apoptosis. *Cell*. 81:505–512.

9. Hsu, H., H.B. Shu, M.G. Pan, and D.V. Goeddel. 1996. TRADD-TRAF2 and TRADD-FADD interactions define two distinct TNF receptor 1 signal transduction pathways. *Cell*. 84:299–308.
10. Micheau, O., and J. Tschopp. 2003. Induction of TNF receptor I-mediated apoptosis via two sequential signaling complexes. *Cell*. 114:181–190.
11. Migone, T.S., J. Zhang, X. Luo, L. Zhuang, C. Chen, B. Hu, J.S. Hong, J.W. Perry, S.F. Chen, J.X. Zhou, et al. 2002. TL1A is a TNF-like ligand for DR3 and TR6/DcR3 and functions as a T cell costimulator. *Immunity*. 16:479–492.
12. Wen, L., L. Zhuang, X. Luo, and P. Wei. 2003. TL1A-induced NF-kB activation and c-IAP2 production prevent DR3-mediated apoptosis in TF-1 cells. *J. Biol. Chem*. 40: 39251–39258.
13. Wang, E.C., J. Kitson, A. Thern, J. Williamson, S.N. Farrow, and M.J. Owen. 2001. Genomic structure, expression, and chromosome mapping of the mouse homologue for the WSL-1 (DR3, Apo3, TRAMP, LARD, TR3, TNFRSF12) gene. *Immunogenetics*. 53:59–63.
14. Warzocha, K., P. Ribeiro, C. Charlot, N. Renard, B. Coiffier, and G. Salles. 1998. A new death receptor 3 isoform: expression in human lymphoid cell lines and non-Hodgkin's lymphomas. *Biochem. Biophys. Res. Commun*. 242:376–379.
15. Yang, C.R., S.L. Hsieh, C.M. Teng, F.M. Ho, W.L. Su, and W.W. Lin. 2004. Soluble decoy receptor 3 induces angiogenesis by neutralization of TL1A, a cytokine belonging to tumor necrosis factor superfamily and exhibiting angiostatic action. *Cancer Res*. 64:1122–1129.
16. Bamias, G., C. Martin III, M. Marini, S. Hoang, M. Mishina, W.G. Ross, M.A. Sachedina, C.M. Friel, J. Mize, S.J. Bickston, et al. 2003. Expression, localization, and functional activity of TL1A, a novel Th1-polarizing cytokine in inflammatory bowel disease. *J. Immunol*. 171:4868–4874.
17. Bamias, G., M. Mishina, M. Nyce, W.G. Ross, G. Kollias, J. Rivera-Nieves, T.T. Pizarro, and F. Cominelli. 2006. Role of TL1A and its receptor DR3 in two models of chronic murine ileitis. *Proc. Natl. Acad. Sci. USA*. 103:8441–8446.
18. Papadakis, K.A., J.L. Prehn, C. Landers, Q. Han, X. Luo, S.C. Cha, P. Wei, and S.R. Targan. 2004. TL1A synergizes with IL-12 and IL-18 to enhance IFN-gamma production in human T cells and NK cells. *J. Immunol*. 172:7002–7007.
19. Wang, E.C., A. Thern, A. Denzel, J. Kitson, S.N. Farrow, and M.J. Owen. 2001. DR3 regulates negative selection during thymocyte development. *Mol. Cell. Biol*. 21:3451–3461.
20. Wills-Karp, M. 2004. Interleukin-13 in asthma pathogenesis. *Curr. Allergy Asthma Rep*. 4:123–131.
21. Meyer, E.H., S. Goya, O. Akbari, G.J. Berry, P.B. Savage, M. Kronenberg, T. Nakayama, R.H. DeKruyff, and D.T. Umetsu. 2006. Glycolipid activation of invariant T cell receptor+ NK T cells is sufficient to induce airway hyperreactivity independent of conventional CD4+ T cells. *Proc. Natl. Acad. Sci. USA*. 103:2782–2787.
22. Sen, Y., B. Yongyi, H. Yuling, X. Luokun, H. Li, X. Jie, D. Tao, Z. Gang, L. Junyan, H. Chunsong, et al. 2005. V alpha 24-invariant NKT cells from patients with allergic asthma express CCR9 at high frequency and induce Th2 bias of CD3+ T cells upon CD226 engagement. *J. Immunol*. 175:4914–4926.
23. Akbari, O., P. Stock, E. Meyer, M. Kronenberg, S. Sidobre, T. Nakayama, M. Taniguchi, M.J. Grusby, R.H. DeKruyff, and D.T. Umetsu. 2003. Essential role of NKT cells producing IL-4 and IL-13 in the development of allergen-induced airway hyperreactivity. *Nat. Med*. 9:582–588.
24. Lisbonne, M., S. Diem, A. de Castro Keller, J. Lefort, L.M. Araujo, P. Hachem, J.M. Fourneau, S. Sidobre, M. Kronenberg, M. Taniguchi, et al. 2003. Cutting edge: invariant V alpha 14 NKT cells are required for allergen-induced airway inflammation and hyperreactivity in an experimental asthma model. *J. Immunol*. 171:1637–1641.
25. Meyer, E.H., M.A. Wurbel, T.L. Staton, M. Pichavant, M.J. Kan, P.B. Savage, R.H. DeKruyff, E.C. Butcher, J.J. Campbell, and D.T. Umetsu. 2007. iNKT cells require CCR4 to localize to the airways and to induce airway hyperreactivity. *J. Immunol*. 179:4661–4671.
26. Terabe, M., J.M. Park, and J.A. Berzofsky. 2004. Role of IL-13 in regulation of anti-tumor immunity and tumor growth. *Cancer Immunol. Immunother*. 53:79–85.
27. Cui, J., T. Shin, T. Kawano, H. Sato, E. Kondo, I. Toura, Y. Kaneko, H. Koseki, M. Kanno, and M. Taniguchi. 1997. Requirement for Valpha14 NKT cells in IL-12-mediated rejection of tumors. *Science*. 278:1623–1626.
28. Godfrey, D.I., and M. Kronenberg. 2004. Going both ways: immune regulation via CD1d-dependent NKT cells. *J. Clin. Invest*. 114: 1379–1388.
29. Van Kaer, L. 2004. Regulation of immune responses by CD1d-restricted natural killer T cells. *Immunol. Res*. 30:139–153.
30. Zhu, Z., R.J. Homer, Z. Wang, Q. Chen, G.P. Geba, J. Wang, Y. Zhang, and J.A. Elias. 1999. Pulmonary expression of interleukin-13 causes inflammation, mucus hypersecretion, subepithelial fibrosis, physiologic abnormalities, and eotaxin production. *J. Clin. Invest*. 103:779–788.
31. Beauvais, F., L. Michel, and L. Dubertret. 1995. Human eosinophils in culture undergo a striking and rapid shrinkage during apoptosis. Role of K+ channels. *J. Leukoc. Biol*. 57:851–855.
32. Schneider, T., D. van Velzen, R. Moqbel, and A.C. Issekutz. 1997. Kinetics and quantitation of eosinophil and neutrophil recruitment to allergic lung inflammation in a brown Norway rat model. *Am. J. Respir. Cell Mol. Biol*. 17:702–712.
33. Yamaguchi, Y., T. Suda, S. Ohta, K. Tominaga, Y. Miura, and T. Kasahara. 1991. Analysis of the survival of mature human eosinophils: interleukin-5 prevents apoptosis in mature human eosinophils. *Blood*. 78:2542–2547.
34. Au-Yeung, B.B., S.D. Katzman, and D.J. Fowell. 2006. Cutting edge: Itk-dependent signals required for CD4+ T cells to exert, but not gain, Th2 effector function. *J. Immunol*. 176:3895–3899.
35. Fowell, D.J., K. Shinkai, X.C. Liao, A.M. Beebe, R.L. Coffman, D.R. Littman, and R.M. Locksley. 1999. Impaired NFATc translocation and failure of Th2 development in Itk-deficient CD4+ T cells. *Immunity*. 11:399–409.
36. Salek-Ardakani, S., J. Song, B.S. Halteman, A.G. Jember, H. Akiba, H. Yagita, and M. Croft. 2003. OX40 (CD134) controls memory T helper 2 cells that drive lung inflammation. *J. Exp. Med*. 198:315–324.
37. Hoshino, A., Y. Tanaka, H. Akiba, Y. Asakura, Y. Mita, T. Sakurai, A. Takaoka, S. Nakaike, N. Ishii, K. Sugamura, et al. 2003. Critical role for OX40 ligand in the development of pathogenic Th2 cells in a murine model of asthma. *Eur. J. Immunol*. 33:861–869.
38. Harhaj, E.W., N.S. Harhaj, C. Grant, K. Mostoller, T. Alefantis, S.C. Sun, and B. Wigdahl. 2005. Human T cell leukemia virus type I Tax activates CD40 gene expression via the NF-kappa B pathway. *Virology*. 333:145–158.
39. Tournoy, K.G., J.C. Kips, and R.A. Pauwels. 2000. Endogenous interleukin-10 suppresses allergen-induced airway inflammation and nonspecific airway responsiveness. *Clin. Exp. Allergy*. 30:775–783.
40. Roh, G.S., S.W. Seo, S. Yeo, J.M. Lee, J.W. Choi, E. Kim, Y. Shin, C. Cho, H. Bae, S.K. Jung, and K. Kwack. 2005. Efficacy of a traditional Korean medicine, Chung-Sang-Bo-Ha-Tang, in a murine model of chronic asthma. *Int. Immunopharmacol*. 5:427–436.
41. Chiba, A., S. Oki, K. Miyamoto, H. Hashimoto, T. Yamamura, and S. Miyake. 2004. Suppression of collagen-induced arthritis by natural killer T cell activation with OCH, a sphingosine-truncated analog of alpha-galactosylceramide. *Arthritis Rheum*. 50:305–313.